

See discussions, stats, and author profiles for this publication at: <https://www.researchgate.net/publication/242488295>

# Synthesis and Micellization Properties of Double Hydrophilic A<sub>2</sub>BA<sub>2</sub> and A<sub>4</sub>BA<sub>4</sub> Non-Linear Block Copolymers

ARTICLE in *MACROMOLECULES* · OCTOBER 2006

Impact Factor: 5.8 · DOI: 10.1021/ma061934w

CITATIONS

62

READS

21

6 AUTHORS, INCLUDING:



Jian Xu

337 PUBLICATIONS 6,819 CITATIONS

SEE PROFILE



Zhishen Ge

University of Science and Technology of China

44 PUBLICATIONS 1,903 CITATIONS

SEE PROFILE



Shizhong Luo

University of Science and Technology of China

24 PUBLICATIONS 937 CITATIONS

SEE PROFILE



Hewen Liu

University of Science and Technology of China

58 PUBLICATIONS 1,064 CITATIONS

SEE PROFILE

# Synthesis and Micellization Properties of Double Hydrophilic A<sub>2</sub>BA<sub>2</sub> and A<sub>4</sub>BA<sub>4</sub> Non-Linear Block Copolymers

Jian Xu, Zhishen Ge, Zhiyuan Zhu, Shizhong Luo, Hewen Liu, and Shiyong Liu\*

Department of Polymer Science and Engineering, Hefei National Laboratory for Physical Sciences at Microscale, University of Science and Technology of China, Hefei, Anhui, 230026, China

Received August 21, 2006; Revised Manuscript Received September 14, 2006

**ABSTRACT:** We describe the first account of the synthesis and intriguing micellization properties of nonlinear double hydrophilic block copolymers (DHBCs) of the A<sub>2</sub>BA<sub>2</sub> and A<sub>4</sub>BA<sub>4</sub> type. Atom transfer radical polymerization (ATRP) macroinitiators with two and four initiating sites at both ends of poly(propylene oxide) (PPO) chain were synthesized via reacting 2-hydroxyethyl acrylate and glycidol with commercially available diamine-terminated PPO, respectively, followed by esterification with excess 2-bromoisobutyl bromide or 2-bromopropionyl bromide. Well-defined nonlinear DHBCs, (PDEA)<sub>2</sub>PPO(PDEA)<sub>2</sub> (H-shaped) and (PDEA)<sub>4</sub>PPO(PDEA)<sub>4</sub> (star-*b*-linear-*b*-star), were then prepared by polymerizing 2-(diethylamino)ethyl methacrylate (DEA) via ATRP in 2-propanol at 40 °C using the prepared macroinitiators, where PDEA was poly(2-(diethylamino)ethyl methacrylate). The structures of the resulting nonlinear shaped copolymers were characterized by <sup>1</sup>H NMR and gel permeation chromatography (GPC). The pH- and thermoresponsive micellization behavior of (PDEA<sub>10</sub>)<sub>2</sub>PPO(PDEA<sub>10</sub>)<sub>2</sub> and (PDEA<sub>11</sub>)<sub>4</sub>PPO(PDEA<sub>11</sub>)<sub>4</sub> was then investigated by a combination of dynamic laser light scattering (LLS) and fluorescence techniques. Compared to the linear counterpart, the nonlinear block copolymers exhibited complex and interesting micellization properties.

## Introduction

Because of their potential applications in pharmaceuticals, coatings, rheology modifiers, colloidal stabilization, and templates for the preparation of nanomaterials, the micellization behavior of amphiphilic block copolymers in aqueous media has received a great deal of attention during the past several decades.<sup>1–18</sup> Double hydrophilic block copolymers (DHBCs) represent a new class of amphiphilic block copolymers, which can self-assemble into one or more types of micelles in water if external conditions such as temperature, pH, and ionic strength are finely tuned.<sup>1,13</sup>

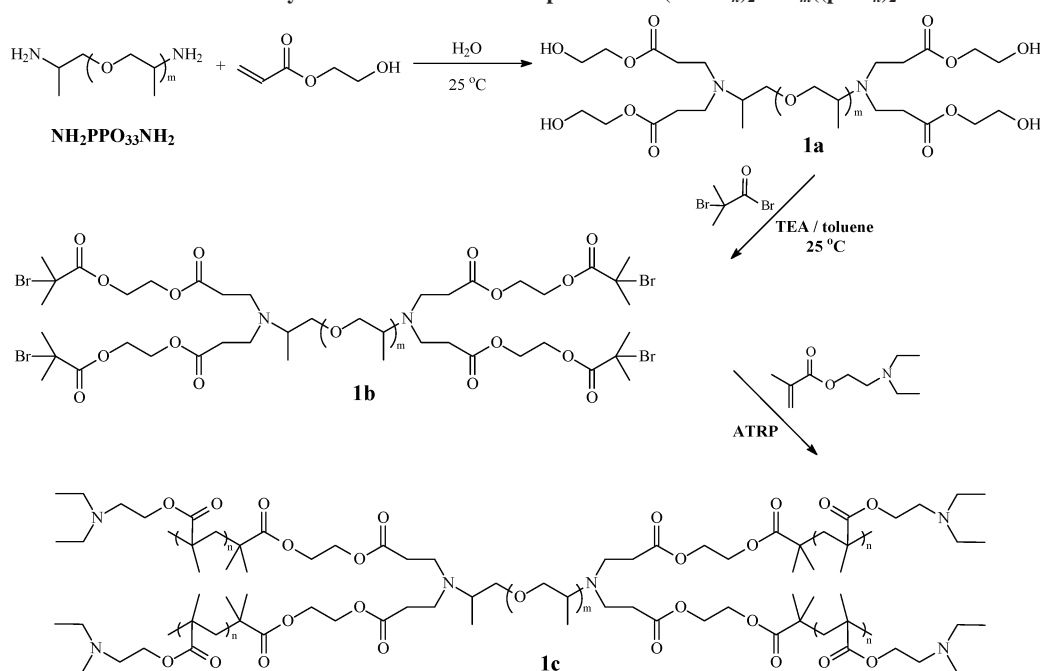
Past studies of DHBCs mainly focused on linear block copolymers.<sup>19</sup> The critical micellization concentration (cmc), the aggregation number (*N*<sub>agg</sub>), the shape, and size of the micelles are mainly determined by the external solution conditions, the composition and molecular weights of DHBCs. Polymer architectures also play a quite important role in determining the micellization properties.<sup>20–22</sup> For example, Hadjichristidis et al.<sup>23</sup> prepared super-H-shaped block copolymers of the PI<sub>3</sub>-PSPI<sub>3</sub> type, where PI is protonated polyisoprene and PS is polystyrene. The micellization behavior of these block copolymers with different PS contents was investigated in *n*-decane, which is a selective solvent for the PI arms. It was found that super-H block copolymers with a large fraction (≥33 mol %) of PS aggregated into near monodisperse, spherical micelles; however, those with a small PS content (≤14 mol %) were nonaggregated under the same conditions. The nonaggregated state should correspond to unimolecular micelles because the central PS block will surely collapse. In comparison with PS/PI linear diblock copolymers, the solubility of PI<sub>3</sub>PSPI<sub>3</sub> in *n*-decane was appreciably enhanced and the micelle aggregation number was ~1 order of magnitude smaller. Pispas et al.<sup>20,21</sup> studied the micellization properties of PS(PI)<sub>2</sub> Y-shaped block

copolymers and (PSPI)<sub>8</sub> star block copolymers, they reported that the nonlinear block copolymers exhibited fundamentally different micellization properties compared to the linear PS-*b*-PI block copolymers.

Recently Armes et al.<sup>24,25</sup> reported the preparation of the first example of stimulus-responsive Y-shaped (AB)<sub>2</sub> DHBCs, which can self-assemble into micelles with different dimensions compared to those formed by the linear diblock copolymers. Compared to the Y-shaped AB<sub>2</sub> block copolymers, an H-shaped block copolymer of the A<sub>2</sub>BA<sub>2</sub> type can be considered as the covalent linkage of the A block between two AB<sub>2</sub> block copolymers. Super-H-shaped block copolymer (A<sub>3</sub>BA<sub>3</sub>) can accordingly be considered as the linkage between two AB<sub>3</sub> block copolymers. A<sub>*n*</sub>BA<sub>*n*</sub> with *n* > 3 should be called star-*b*-linear-*b*-star block copolymers or pom-pom polymers.<sup>22,26,27</sup>

The syntheses of nonlinear shaped A<sub>*n*</sub>BA<sub>*n*</sub> (*n* ≥ 2) block copolymers typically rely on the anionic polymerization technique, which is always challenging due to the time-consuming purification of monomers, the unavoidable side reactions, and the necessity of quantitative addition of each reactant. Hadjichristidis et al.<sup>22,26,27</sup> and Knauss et al.<sup>28,29</sup> have worked extensively on this subject and presented some nice examples.<sup>30–32</sup> With the advent of controlled/living free radical polymerizations, such as nitroxide-mediated polymerization (NMP),<sup>33</sup> reversible addition–fragmentation chain transfer (RAFT),<sup>34,35</sup> and atom transfer radical polymerization (ATRP),<sup>36,37</sup> the syntheses of A<sub>*n*</sub>-BA<sub>*n*</sub> (*n* ≥ 2) block copolymers can be conducted in a much simpler manner through successive controlled free radical polymerizations or its combination with conventional living polymerization techniques such as cationic ring-opening polymerization and anionic polymerization.<sup>26</sup> Pan et al.<sup>38–40</sup> reported the synthesis of H-shaped (PS)<sub>2</sub>PEO(PS)<sub>2</sub> via ATRP and the preparation of (PDOP)<sub>2</sub>PS(PDOP)<sub>2</sub> through a combination of RAFT and ring-opening polymerization, where PEO was poly(ethylene oxide) and PDOP is poly(1,3-dioxepane).<sup>41</sup> Just recently, An et al.<sup>42</sup> reported the preparation of asymmetric H-shaped (PS)<sub>2</sub>PEO(PMMA)<sub>2</sub> block copolymers via a combina-

\* To whom correspondence should be addressed. Email: slui@ustc.edu.cn

Scheme 1. Synthetic Route for the Preparation of  $(\text{PDEA}_n)_2\text{PPO}_m((\text{pdea}_n)_2)$ 

tion of ATRP and living anionic polymerization, which represented a new development in the family of H-shaped block copolymers. Hizal et al.<sup>43</sup> combined the Diels–Alder reaction with controlled/living free radical polymerization to prepare heteroarm H-shaped block copolymers. Just recently, Monteiro et al.<sup>44</sup> successfully prepared three-miktoarm star copolymers and H-shaped block copolymers using a combination of ATRP and “click” chemistry, which provided to be a more straightforward approach for the preparation of block copolymers with different chain architectures.

To the best of our knowledge, the syntheses and stimuli-responsive self-assembly behavior of DHBCs of the nonlinear  $A_nBA_n$  ( $n \geq 2$ ) type have not been reported yet. It is well-known that poly(propylene oxide) (PPO) with a molar mass of  $\sim 2000$  g/mol molecularly dissolves in cold, dilute aqueous solution but becomes insoluble at  $\sim 20$  °C and its lower critical solution temperature (LCST) lies between 10 and 20 °C, depending on the solution concentrations; while poly(2-(diethylamino)ethyl methacrylate) (PDEA) homopolymer is soluble in acidic solution as a weak cationic polyelectrolyte due to protonation of the tertiary amine residues but precipitates from solution at around neutral pH. We have previously reported the micellization of PPO-*b*-PDEA linear diblock copolymer in aqueous solution.<sup>45</sup> PDEA-core micelles were formed at 5 °C in mildly alkaline solution (pH 8.5), and PPO-core micelles were obtained at pH 6.5 at elevated temperatures (40–70 °C).<sup>45</sup>

In this work, we reported the synthesis and micellization properties of novel nonlinear DHBCs of the  $A_2BA_2$  and  $A_4BA_4$  type, i.e., the H-shaped  $(\text{PDEA})_2\text{PPO}(\text{PDEA})_2$  and the star-*b*-linear-*b*-star type  $(\text{PDEA})_4\text{PPO}(\text{PDEA})_4$  block copolymers. ATRP macroinitiators with two and four initiating sites at both ends of the PPO chain were prepared at first; well-defined nonlinear shaped DHBCs were then synthesized by polymerizing 2-(diethylamino)ethyl methacrylate (DEA) in 2-propanol at 40 °C using these macroinitiators. The pH-responsive and thermoresponsive micellization behavior of  $(\text{PDEA})_2\text{PPO}(\text{PDEA})_2$  and  $(\text{PDEA})_4\text{PPO}(\text{PDEA})_4$  was then investigated by a combination of dynamic light scattering (LLS) and fluorescence techniques. Subsequently, a comparison of the micellization

behavior of the linear and nonlinear block copolymers was made.

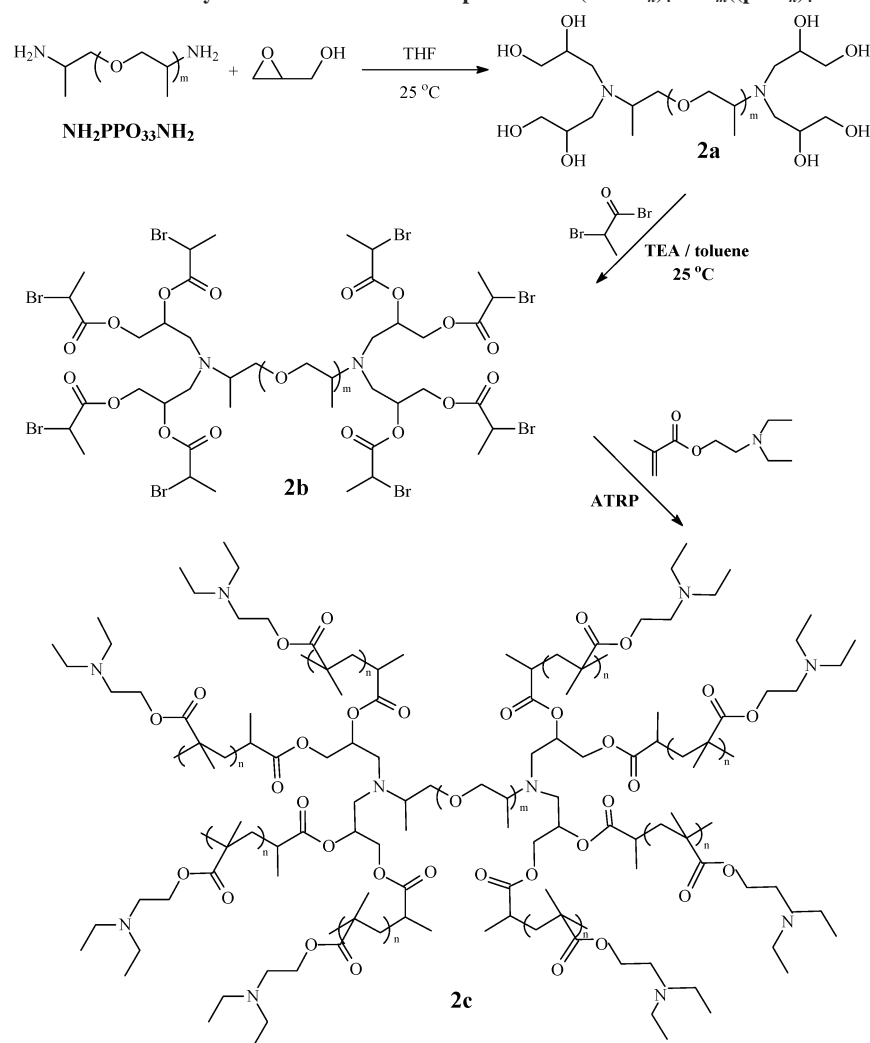
## Experimental Section

**Materials.** Poly(propylene oxide) bis(2-aminopropyl ether) ( $\text{NH}_2\text{—PPO}_{33}\text{—NH}_2$ ) with a nominated number-average molecular weight,  $M_n$ , of 2000 (with a degree of polymerization (DP) of 33) and a polydispersity index,  $M_w/M_n$ , of 1.1 was purchased from Aldrich, it was further purified by passing through a neutral alumina column and dried under vacuum. Glycidol (Fluka, 99%) was dried over molecular sieves and distilled twice under reduced pressure prior to use. 2-hydroxyethyl acrylate (HEA, 99%), 2-(diethylamino)ethyl methacrylate (DEA, 99%), 2-bromoisobutyryl bromide (98%), 2-bromopropionyl bromide (97%), copper(I) bromide ( $\text{CuBr}$ , 99.999%) and 2,2'-bipyridine (bpy,  $\geq 99\%$  purity) were all purchased from Aldrich. All monomers were passed through silica columns prior to their use. All other chemicals were purchased from Shanghai Experiment Reagent Co., Ltd.

**Synthesis.** The general synthetic route for the preparation of H-shaped  $(\text{PDEA})_2\text{PPO}(\text{PDEA})_2$  and  $(\text{PDEA})_4\text{PPO}(\text{PDEA})_4$  star-*b*-linear-*b*-star block copolymers were shown in Schemes 1 and 2, respectively.

**Synthesis of  $\text{Br}_2\text{—PPO}_{33}\text{—Br}_2$  Macroinitiator (1b).**  $\text{NH}_2\text{—PPO}_{33}\text{—NH}_2$  (20.0 g, 0.01 mol), HEA (7.0 g, 0.06 mol),  $[\text{HEA}]/[\text{NH}_2] = 6.0$ , deionized water (1.0 g), and hydroquinone (10 mg) were added to a 100 mL one-necked round-bottomed flask. The reaction mixture was stirred at room temperature for 3 days.  $^1\text{H}$  NMR studies indicated that the Michael addition went to completion.<sup>24,25</sup> Excess HEA and water was removed under reduced pressure. 200 mL of chloroform was added, the solution was thoroughly washed with  $3 \times 100$  mL of saturated  $\text{NaHCO}_3$  solution. The organic layer was collected and dried over anhydrous  $\text{MgSO}_4$ . After removing the solvent, the obtained  $\text{OH}_2\text{PPO}_{33}\text{OH}_2$  (**1a**) was dried under vacuum overnight at room temperature.

The ATRP macroinitiator (**1b**),  $\text{Br}_2\text{PPO}_{33}\text{Br}_2$ , was obtained by the esterification of **1a** with excess 2-bromoisobutyryl bromide.<sup>46</sup> **1a** ( $5 \times 10^{-3}$  mol) was dissolved in 150 mL toluene, after azeotropic distillation of 20–30 mL of toluene under reduced pressure to remove traces of water, dry triethylamine (0.03 mol) was added, and the solution was cooled to 0 °C. 2-bromoisobutyryl bromide (0.03 mol) was added dropwise via a dropping funnel over 2 h, the reaction mixture was then stirred overnight at room temperature. The precipitated salt was removed by filtration, and most of the

Scheme 2. Synthetic Route for the Preparation of  $(\text{PDEA}_n)_4\text{PPO}_m((\text{pdea}_n)_4)$ 

solvent was removed by rotary evaporation. The crude product was dissolved in dichloromethane and washed 3 times with saturated  $\text{NaHCO}_3$  solution. The organic solution was collected and dried over anhydrous  $\text{MgSO}_4$ . The solvent was then removed, and the obtained **1b** was dried under vacuum overnight at room temperature.

**Synthesis of  $\text{Br}_4\text{—PPO}_{33}\text{—Br}_4$  Macroinitiator (**2b**).**  $\text{NH}_2\text{PPO}_{33}\text{—NH}_2$  was used as the starting material again for the preparation of **2b**. Glycidol (20.0 mmol) was added dropwise into 5.0 g of  $\text{NH}_2\text{PPO}_{33}\text{—NH}_2$  (2.5 mmol) with ice cooling, then the mixture was reacted for 2 h at  $25^\circ\text{C}$ .<sup>47–49</sup> Subsequently the unreacted glycidol were removed under reduced pressure. The product was dried at  $40^\circ\text{C}$  under vacuum for 24 h, affording 5.72 g of **2a**. The ATRP macroinitiator **2b**,  $\text{Br}_4\text{PPO}_{33}\text{Br}_4$ , was obtained by the esterification of  $\text{HO}_4\text{PPO}_{33}\text{OH}_4$  with excess 2-bromopropionyl bromide following similar procedures used for the preparation of **1b**.

**Synthesis of Nonlinear H-Shaped and Star-*b*-Linear-*b*-Star Block Copolymers.** A typical example for the preparation of  $(\text{PDEA})_4\text{PPO}(\text{PDEA})_4$  was described below. The ATRP macroinitiator **2b** (0.1 mmol, 0.8 mmol initiating sites), DEA (10 mmol), bpy (0.8 mmol), and 2-propanol (equal volume to the DEA monomer) were added to a reaction flask and the solution was degassed by three freeze–thaw cycles. After the solution temperature was increased to  $40^\circ\text{C}$ , CuBr (0.4 mmol) was introduced as a solid into the reaction flask under  $\text{N}_2$  atmosphere to start the polymerization. The reaction solution became more viscous as polymerization proceeded. After about 6 h the conversion was  $\sim 80\%$  as judged by  $^1\text{H}$  NMR. The reaction mixture was diluted with 2-propanol and passed through a silica column to remove residual copper catalysts. After the solvent was removed, the crude product was extracted with ice-cold water ( $0^\circ\text{C}$ , pH 9) several

times to remove possible traces of PPO. The white viscous solids were then dried in a vacuum oven to afford **2c**. The preparation of  $(\text{PDEA})_2\text{PPO}(\text{PDEA})_2$ , **1c**, followed the same procedure used for the preparation of **2c** except that the amount of monomer, solvent, and catalysts were halved, a typical conversion of  $\sim 90\%$  was achieved in 4 h.

**Nuclear Magnetic Resonance (NMR) Spectroscopy.**  $^1\text{H}$  NMR spectra were recorded on a Bruker DMX-300 nuclear magnetic resonance (NMR) instrument with  $\text{CDCl}_3$  as solvent and tetramethylsilane (TMS) as the internal standard.

**Gel Permeation Chromatography (GPC).** The molecular weight and molecular weight distribution of the polymers were measured using a Waters 150  $^\circ\text{C}$  gel permeation chromatography (GPC) system equipped with microStyragel columns (500,  $10^3$ , and  $10^4$  Å) and Waters RI detector at  $30^\circ\text{C}$ . Molecular weights were calibrated against low polydispersity polystyrene standards. THF was used as the eluent at a flow rate of 1.0 mL/min.

**Laser Light Scattering (LLS).** A commercial spectrometer (ALV/DLS/SLS-5022F) equipped with a multi- $\tau$  digital time correlation (ALV5000) and a cylindrical 22 mW UNIPHASE He–Ne laser ( $\lambda_0 = 632$  nm) as the light source was used. In dynamic LLS, the Laplace inversion of each measured intensity–intensity–time correlation function  $G^{(2)}(q, t)$  in the self-beating mode can lead to a line-width distribution  $G(\Gamma)$ . For a pure diffusive relaxation,  $\Gamma$  is related to the translational diffusion coefficient  $D$  by  $(\Gamma/q^2)_{C \rightarrow 0, q \rightarrow 0} \rightarrow D$ , or further to the hydrodynamic radius  $R_h$  via the Stokes–Einstein equation,  $R_h = (k_B T / 6\pi\eta_0) / D$ , where  $k_B$ ,  $T$ , and  $\eta_0$  are the Boltzmann constant, the absolute temperature, and the solvent viscosity, respectively.



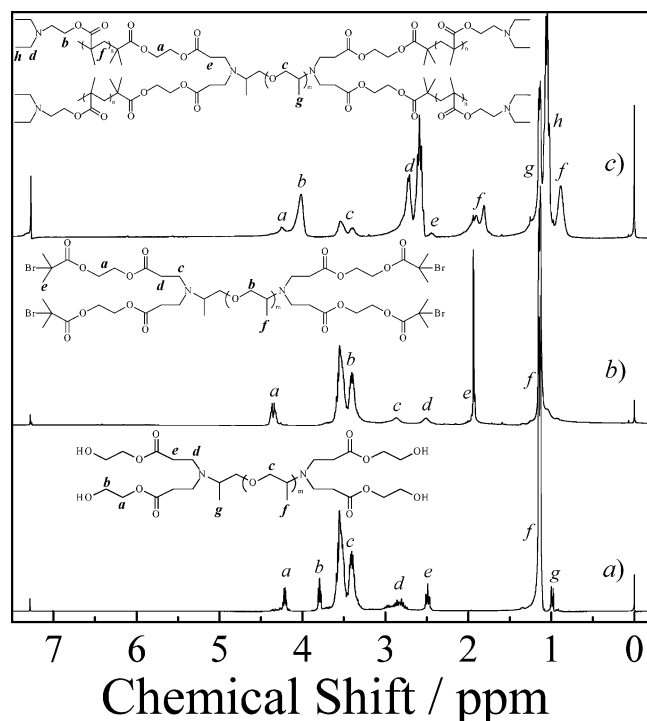


**Figure 1.**  $^1\text{H}$  NMR spectra: (a) **1a**, (b) **1b**,  $(\text{Br})_2\text{PPO}_{33}(\text{Br})_2$ , and (c) **1c**,  $(\text{PDEA})_2\text{PPO}_{33}(\text{PDEA})_2$ .

**Fluorescence Measurements.** Fluorescence spectra were recorded using a JASCO FP-6200 spectrofluorimeter. The temperature of the water-jacketed cell holder was controlled by a programmable circulation bath. The slit widths were set at 5.0 nm for both the excitation and the emission. The critical micellization temperature was determined by fluorescence technique. Calculated volumes of pyrene solution in acetone was added into a series of volumetric flasks, acetone was removed under reduced pressure, polymer solutions at a concentration of 0.5 wt % were then added into volumetric flasks, pyrene concentration was fixed at  $5 \times 10^{-7}$  mol/L. All the samples were sonicated for 2 h and then allowed to stand overnight before fluorescence measurements.

## Results and Discussion

**The General Synthetic Routes Used for the Preparation of H-Shaped Polymers.**  $(\text{PDEA})_2\text{PPO}(\text{PDEA})_2$  and  $(\text{PDEA})_4\text{PPO}(\text{PDEA})_4$  star-*b*-linear-*b*-star block copolymers are shown in Schemes 1 and 2, respectively. The first step involved in the preparation of ATRP macroinitiators, **1b** and **2b**, was the addition reaction of the terminal primary amine groups of  $\text{NH}_2\text{-PPO-NH}_2$  with HEA or glycidol, forming multihydroxyl terminated PPO (**1a** and **2a**). The second step was the esterification of terminal hydroxyl groups of **1a** and **2a** with excess 2-bromoisobutyryl bromide or 2-bromopropionyl bromide, resulting in the ATRP macroinitiators **1b** and **2b**. The final step was the polymerization of DEA monomer via ATRP using **1b** and **2b**.

**Addition Reaction of  $\text{NH}_2\text{PPO}_{33}\text{NH}_2$  and HEA/Glycidol.** During the Michael addition reaction between  $\text{NH}_2\text{PPO}_{33}\text{NH}_2$  and HEA, an excess of HEA was added considering that one primary amine group will react with 2 molecules of HEA. Water (5.0 wt % relative to  $\text{NH}_2\text{PPO}_{33}\text{NH}_2$ ) was added to accelerate this reaction.<sup>24,25</sup> The Michael addition reaction went to completion under our conditions. This was confirmed by the  $^1\text{H}$  NMR spectrum of **1a** (Figure 1a). No residual acryloyl signals at  $\delta = 5.7\text{--}6.5$  ppm can be detected, indicating that excess HEA was completely removed. The peaks at 4.1–4.3 ppm (a) and 3.7–3.8 ppm (b) were ascribed to the protons of ester methylene of HEA and the methylene protons next to hydroxyl group. The

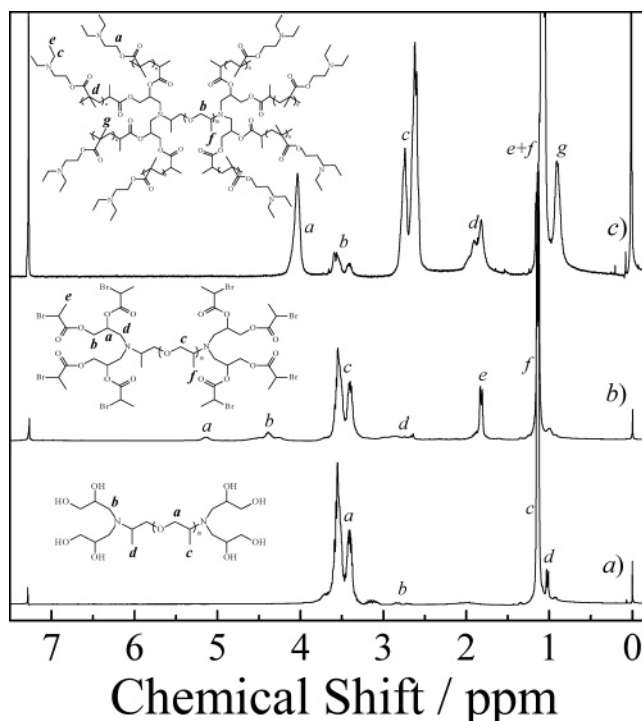


**Figure 2.**  $^1\text{H}$  NMR spectra: (a) **2a**, (b) **2b**,  $(\text{Br})_4\text{PPO}_{33}(\text{Br})_4$ , and (c) **2c**,  $(\text{PDEA})_4\text{PPO}_{33}(\text{PDEA})_4$ .

resonances at  $\delta = 2.7\text{--}2.9$  ppm (d), 2.4–2.5 ppm (e) were ascribed to protons on the new bonds formed from the addition reaction of amine group and the double bond of HEA. Peak g at 0.9–1.0 ppm corresponded to the methyl groups of PPO. The ratio of integrals of peak a to c was  $\sim 1/50$ , this plus the fact that the integration ratio of peak b:e:g = 4:4:3 led us to conclude that that starting material,  $\text{NH}_2\text{PPO}_{33}\text{NH}_2$ , was quantitatively transformed into **1a**.

The addition reaction between  $\text{NH}_2\text{PPO}_{33}\text{NH}_2$  and glycidol afforded **2a** under stated conditions.<sup>47–49</sup> The mass increase after the reaction was  $\sim 14.4\%$ , indicating that the addition reaction is quantitative and went to nearly 100% conversion.

**Esterification of **1a** and **2a**.** To ensure the complete transformation of **1a** and **2a** into **1b** and **2b**, excess of 2-bromoisobutyryl bromide or 2-bromopropionyl bromide was used, which can be easily removed by washing with saturated  $\text{NaHCO}_3$  aqueous solution. During the preparation of **2b**, 2-bromopropionyl bromide was intentionally chosen for the esterification of **2a** considering that the 8 terminal bromine groups will be less sterically hindered. However, preliminary experiments revealed that the esterification of **2a** with 2-bromoisobutyryl bromide produced ATRP initiators with comparable initiating efficiencies. The spectrum of **1b** is shown in Figure 1b. In comparison with the  $^1\text{H}$  NMR spectrum of **1a**, the signals at  $\delta = 3.7\text{--}3.8$  ppm ( $\text{CH}_2\text{OH}$ ) completely disappeared in the  $^1\text{H}$  NMR spectrum of **1b**. The new resonances at  $\delta = 1.9$  ppm (e) was due to the methyl groups of the two bromoisobutyryl groups located at both ends of **1b**. The degree of esterification was calculated to be  $\sim 98\%$  by comparing the integrals of peak e to peak b.

The reaction between **2a** and excess 2-bromopropionyl bromide resulted in the formation of **2b**, and its  $^1\text{H}$  NMR spectrum is shown in Figure 2b. The signal at  $\delta = 5.1$  ppm (a) was ascribed to the ester methine protons, and the signal at  $\delta = 4.2\text{--}4.5$  ppm (b) was ascribed to the ester methylene protons. The signal at  $\delta = 1.8\text{--}1.9$  ppm (e) corresponded to the methyl protons of the end bromopropionyl groups. The degree of

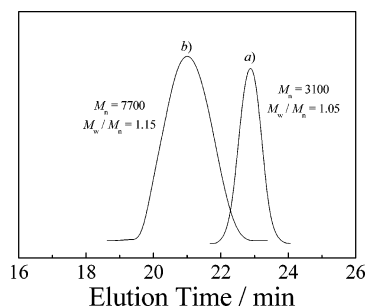


**Figure 3.** GPC traces of (a) ATRP macroinitiator **1b** and (b) (PDEA<sub>10</sub>)<sub>2</sub>PPO-(PDEA<sub>10</sub>)<sub>2</sub> block copolymer **1c**. Reaction conditions: [DEA]:[**1b**]:[CuBr]:[bpy] = 100:1:2:4, 2-propanol, 40 °C.

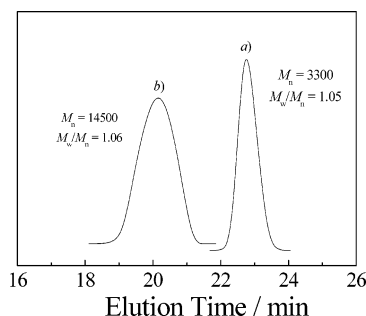


**Figure 4.** GPC traces of (a) ATRP macroinitiator **2b** and (b) (PDEA<sub>11</sub>)<sub>4</sub>PPO-(PDEA<sub>11</sub>)<sub>4</sub> block copolymer **2c**. Reaction conditions: [DEA]:[**2b**]:[CuBr]:[bpy] = 100:1:4:8, 2-propanol, 40 °C.

esterification was calculated to be ~97% by comparing the integrals of peak *e* to peak *c*.

**ATRP Polymerization of DEA Using **1b** and **2b** as Macroinitiators.** **1b** and **2b** were then employed as multifunctional initiators for the ATRP polymerization of DEA in the presence of CuBr/bpy catalysts. Since the PPO block is quite short (DP = 33), the length of the PDEA arms needs to be relatively short to observe prominent stimuli-responsive micellization properties. In a typical ATRP polymerization, high catalyst concentration is problematic and will typically generate high concentrations of radicals in the early stages of the polymerization, leading to unwanted termination and reduced control of the polymerization process.<sup>50</sup> For example, for the ATRP polymerization of DEA in 2-propanol at a molar ratio of [DEA]:[Br<sub>4</sub>PPO<sub>33</sub>Br<sub>4</sub>]:[CuBr]:[bpy] = 100:1:8:16 (i.e. a mean theoretical DP<sub>n</sub> of 12 for each PDEA block), GPC analysis of samples at 90% conversion (determined by <sup>1</sup>H NMR analysis, achieved within 4 h at 40 °C) revealed an *M<sub>n</sub>* of 21 600 and an *M<sub>w</sub>/M<sub>n</sub>* of 1.43, with a small tail at the low molecular weight side. This suggested that partial radical coupling occurred in the early stages of polymerization. In marked contrast, at a molar ratio of [DEA]:[Br<sub>4</sub>PPO<sub>33</sub>Br<sub>4</sub>]:[CuBr]:[bpy] = 100:1:4:8 under the same conditions, the DEA conversion reached ~80% after 6 h and a significantly lower polydispersity of 1.06 was obtained. Thus, ATRP polymerization of DEA using **1b** and **2b** macroinitiators can be reasonably well controlled even at relatively low target degrees of polymerization provided that lower catalyst concentration was employed.

Typical GPC traces of (PDEA)<sub>2</sub>PPO(PDEA)<sub>2</sub> and (PDEA)<sub>4</sub>PPO(PDEA)<sub>4</sub> were shown in Figures 3 and 4, respectively. Both GPC curves (Figure 3b, 4b) were monomodal and quite symmetric, indicating that well-defined nonlinear A<sub>n</sub>BA<sub>n</sub> block copolymers were obtained. If the A<sub>n</sub>BA<sub>n</sub> block copolymers contain 2*n*, 2*n* - 1, and 2*n* - 2 branches, which may occur due to the intramolecular irreversible termination reactions or the inefficient initiation during polymerization, the GPC curve

**Table 1.** Summary of Molecular Parameters of the A<sub>n</sub>BA<sub>n</sub> Block Copolymers

sample	<i>M<sub>n</sub></i> , GPC	<i>M<sub>w</sub>/M<sub>n</sub></i>	<i>M<sub>n</sub></i> , NMR	<i>M<sub>n</sub></i> , th <sup>a</sup>
(PDEA <sub>10</sub> ) <sub>2</sub> PPO <sub>33</sub> (PDEA <sub>10</sub> ) <sub>2</sub>	7700	1.15	10 700	10 500
(PDEA <sub>11</sub> ) <sub>4</sub> PPO <sub>33</sub> (PDEA <sub>11</sub> ) <sub>4</sub>	14 500	1.06	19 800	19 300

<sup>a</sup> *M<sub>n</sub>*, th = ([*M*]<sub>0</sub>/[*I*]<sub>0</sub>) × conversion × 185 + *M<sub>n</sub>*, PPO, where [*M*]<sub>0</sub> and [*I*]<sub>0</sub> are the feed molar concentrations of DEA and initiating sites, 185 and *M<sub>n</sub>*, PPO are the molecular weights of DEA monomer and PPO macroinitiators.

will exhibit a tail at the lower molecular weight side. We can at least conclude that the major products were the desired nonlinear H-shaped and star-*b*-linear-*b*-star block copolymers.<sup>38,42</sup>

The actual DP of the PDEA branches of the nonlinear block copolymers **1c** and **2c** were determined by <sup>1</sup>H NMR. The <sup>1</sup>H NMR spectra of (PDEA)<sub>2</sub>PPO(PDEA)<sub>2</sub> and (PDEA)<sub>4</sub>PPO(PDEA)<sub>4</sub> are shown in Figure 1c and Figure 2c, respectively. Taking (PDEA)<sub>2</sub>PPO(PDEA)<sub>2</sub> as an example (Figure 1c), the molar composition of the copolymer can be determined from the relative integral ratio of peaks at δ = 3.3–3.7 ppm (*c*) (–CH<sub>2</sub>CH(CH<sub>3</sub>)O– of the PPO block) to that at δ = 4.0 ppm (*b*) (–OCH<sub>2</sub>CH<sub>2</sub>N– of the PDEA block). *M<sub>n</sub>*, NMR of the H-shaped block copolymers can then be calculated as follows:

$$M_{n,NMR} = M_{n,PPO} + \frac{M_{n,PPO}}{58} \times \frac{3I_b}{2I_c} \times 185 \quad (1)$$

where *M<sub>n</sub>*, PPO, 58, and 185 denote the molecular weights of PPO block, propylene oxide, and DEA monomer, respectively. *I<sub>b</sub>* and *I<sub>c</sub>* were the integrals of peaks *b* and *c*.

We can then determine the DP of the PDEA branches. Table 1 summarizes the molecular parameters of the H-shaped and star-*b*-linear-*b*-star block copolymers. (PDEA<sub>10</sub>)<sub>2</sub>PPO<sub>33</sub>(PDEA<sub>10</sub>)<sub>2</sub> and (PDEA<sub>11</sub>)<sub>4</sub>PPO<sub>33</sub>(PDEA<sub>11</sub>)<sub>4</sub> were successfully obtained. It was found that the theoretical molecular weight, *M<sub>n</sub>*, th, is quite close to *M<sub>n</sub>*, NMR. We can also see that *M<sub>n</sub>*, GPC is systematically lower than that of *M<sub>n</sub>*, NMR, reflecting the topological effects on the hydrodynamic volumes of the nonlinear shaped block copolymers (which is typically smaller) as compared to their linear counterpart. The determination of the molar masses of nonlinear block copolymers by GPC is not straightforward. The calibration with narrow standards cannot be applied, as standard samples with exactly the same topology and with known molar masses do not exist.

**Micellization Properties.** Previously we reported the “schizophrenic” micellization behavior of PPO<sub>33</sub>-*b*-PDEA<sub>42</sub> in dilute aqueous solution.<sup>45</sup> Due to the thermoresponsive solubility of PPO block and the pH-responsive solubility of PDEA block, two micellar states existed in water under different solution conditions. At pH 8.5 and 5 °C, PDEA-core micelles with an average hydrodynamic radius, <R<sub>h</sub>>, of 40 nm were formed, and at pH 6.5 and 40 °C, PPO-core micelles with a <R<sub>h</sub>> of 84 nm were formed. It should be noted that PPO<sub>33</sub>-*b*-PDEA<sub>42</sub> and (PDEA<sub>10</sub>)<sub>2</sub>PPO<sub>33</sub>(PDEA<sub>10</sub>)<sub>2</sub> have comparable PPO molar contents. Thus, the obtained (PDEA<sub>10</sub>)<sub>2</sub>PPO<sub>33</sub>(PDEA<sub>10</sub>)<sub>2</sub> and (PDEA<sub>11</sub>)<sub>4</sub>PPO<sub>33</sub>(PDEA<sub>11</sub>)<sub>4</sub> provided to be good candidates for studying the chain architectural effects on the micellization behavior of DHBCs.

Both nonlinear DHBCs, (PDEA<sub>10</sub>)<sub>2</sub>PPO<sub>33</sub>(PDEA<sub>10</sub>)<sub>2</sub> and (PDEA<sub>11</sub>)<sub>4</sub>PPO<sub>33</sub>(PDEA<sub>11</sub>)<sub>4</sub> molecularly dissolved in dilute aqueous solution at pH 6.5 and 5 °C, which was confirmed by dynamic LLS measurements of 0.5 w/v % solutions. Upon addition of a small amount of NaOH to this solution at 5 °C, micellization occurred at pH 8 or higher, as suggested by the quick appearance of the characteristic bluish tinge. Figure 5

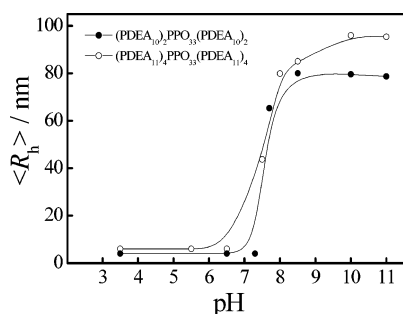


**Figure 5.** Variation of hydrodynamic radius,  $\langle R_h \rangle$ , as a function of solution pH for (PDEA<sub>10</sub>)<sub>2</sub>PPO<sub>33</sub>(PDEA<sub>10</sub>)<sub>2</sub> and (PDEA<sub>11</sub>)<sub>4</sub>PPO<sub>33</sub>(PDEA<sub>11</sub>)<sub>4</sub> block copolymers at a concentration of 0.5 wt % and 5 °C. The scattering angle is 90°.

showed the variation of  $\langle R_h \rangle$  as a function of solution pH for (PDEA<sub>10</sub>)<sub>2</sub>PPO<sub>33</sub>(PDEA<sub>10</sub>)<sub>2</sub> and (PDEA<sub>11</sub>)<sub>4</sub>PPO<sub>33</sub>(PDEA<sub>11</sub>)<sub>4</sub> at a concentration of 0.5 wt % and 5 °C. At pH 10, dynamic LLS revealed  $\langle R_h \rangle$  values of 80 and 96 nm for (PDEA<sub>10</sub>)<sub>2</sub>PPO<sub>33</sub>(PDEA<sub>10</sub>)<sub>2</sub> and (PDEA<sub>11</sub>)<sub>4</sub>PPO<sub>33</sub>(PDEA<sub>11</sub>)<sub>4</sub> block copolymers, respectively. The polydispersity indexes ( $\mu_2/\Gamma^2$ ) were 0.08 and 0.06 by cumulants analysis, respectively. In agreement with the LLS results, <sup>1</sup>H NMR studies of (PDEA<sub>10</sub>)<sub>2</sub>PPO<sub>33</sub>(PDEA<sub>10</sub>)<sub>2</sub> in D<sub>2</sub>O further confirmed the formation of PDEA-core micelles at slightly alkaline solution and 5 °C.<sup>45,46</sup>

A comparison of PPO<sub>33</sub>-*b*-PDEA<sub>42</sub>, (PDEA<sub>10</sub>)<sub>2</sub>PPO<sub>33</sub>(PDEA<sub>10</sub>)<sub>2</sub>, and (PDEA<sub>11</sub>)<sub>4</sub>PPO<sub>33</sub>(PDEA<sub>11</sub>)<sub>4</sub> tells us that the nonlinear block copolymers forms much larger PDEA-core micelles compared to their linear counterpart.<sup>20,21</sup> Moreover, the PDEA-core micelles of (PDEA<sub>11</sub>)<sub>4</sub>PPO<sub>33</sub>(PDEA<sub>11</sub>)<sub>4</sub> is larger than that of (PDEA<sub>10</sub>)<sub>2</sub>PPO<sub>33</sub>(PDEA<sub>10</sub>)<sub>2</sub>, probably due to the higher PDEA contents in the former.<sup>1,51</sup> On the basis of chemical intuition, at alkaline pH conditions and 5 °C, the deprotonated PDEA branches of these two types of nonlinear block copolymers should form hydrophobic micelle cores, with the still-solvated PPO central block forming the micelle corona. A schematic illustration for the formation of PDEA-core micelles from (PDEA)<sub>4</sub>PPO(PDEA)<sub>4</sub> is shown in Figure 6. The soluble central PPO block will form loops around the surface of PDEA-core, i.e., the PDEA-core micelles will take a “flowerlike” structure.<sup>51</sup> However, For the PDEA-core micelles of (PDEA)<sub>4</sub>PPO<sub>33</sub>(PDEA)<sub>4</sub>, a rather large micelle radius of 96 nm was observed. Even if the soluble PPO corona chains were fully stretched,

the star-linear-star block copolymer could not possibly give a spherical micelle with a  $\langle R_h \rangle$  of 96 nm.<sup>22,51</sup> The unusually large micelle size is thus not consistent with a simple core-shell nanostructure. Because of the spatial arrangement of PDEA branches, we can speculate that the PDEA micelle core should be loosely packed. At this stage, we cannot exclude the possibility that these PDEA-core aggregates may be actually compound micelles or vesicles.<sup>19</sup> Regardless of the precise morphology of these aggregates, the pH-induced self-assembly process is fully reversible; i.e., molecularly dissolved copolymer solutions are obtained again upon lowering pH to <6 at 5 °C.

Presumably, heating the unimer solution of (PDEA<sub>10</sub>)<sub>2</sub>PPO<sub>33</sub>(PDEA<sub>10</sub>)<sub>2</sub> and (PDEA<sub>11</sub>)<sub>4</sub>PPO<sub>33</sub>(PDEA<sub>11</sub>)<sub>4</sub> at pH 6.5 and 5 °C will lead to the formation of PPO-core micelles, just as the case of PPO<sub>33</sub>-*b*-PDEA<sub>42</sub> diblock copolymer.<sup>45</sup> Unexpectedly, we found that the scattering light intensities of aqueous solutions of both types of nonlinear DHBCs did not change with increasing temperatures, even at the highest temperature investigated (70 °C). A typical plot for the (PDEA<sub>10</sub>)<sub>2</sub>PPO<sub>33</sub>(PDEA<sub>10</sub>)<sub>2</sub> block copolymer is shown in Figure 7. The variation of scattering intensities with temperatures for PPO<sub>33</sub>-*b*-PDEA<sub>42</sub> is also plotted. This strongly suggested that upon heating of the aqueous solution of (PDEA<sub>10</sub>)<sub>2</sub>PPO<sub>33</sub>(PDEA<sub>10</sub>)<sub>2</sub>, no inter-chain aggregation took place although the central PPO block will become hydrophobic at elevated temperatures. This seemed to be unreasonable considering that both PPO<sub>33</sub>-*b*-PDEA<sub>42</sub> and (PDEA<sub>10</sub>)<sub>2</sub>PPO<sub>33</sub>(PDEA<sub>10</sub>)<sub>2</sub> have comparable PPO molar contents and overall molecular weights. It should be noted that even the LLS studies were conducted at a much higher concentration (2.0 wt %), the scattering intensities still did not change with temperatures for both types of nonlinear block copolymers. So the constant scattering intensities with varying temperatures cannot be due to that the polymer concentration tested is below their critical micellization concentration. We then tentatively proposed that for (PDEA<sub>10</sub>)<sub>2</sub>PPO<sub>33</sub>(PDEA<sub>10</sub>)<sub>2</sub> and (PDEA<sub>11</sub>)<sub>4</sub>PPO<sub>33</sub>(PDEA<sub>11</sub>)<sub>4</sub>, heating their aqueous solutions at pH 6.5 will lead to the formation of unimolecular micelles with the core consisting of a single PPO block (see Figure 6).<sup>23</sup>

In our case, LLS failed to determine the onset of thermoresponsive micellization because the scattering intensities did not change with temperature. Direct determination of the coil size by LLS was not practicable due to the fact that large errors will be incurred when measuring sizes down to a few nanom-

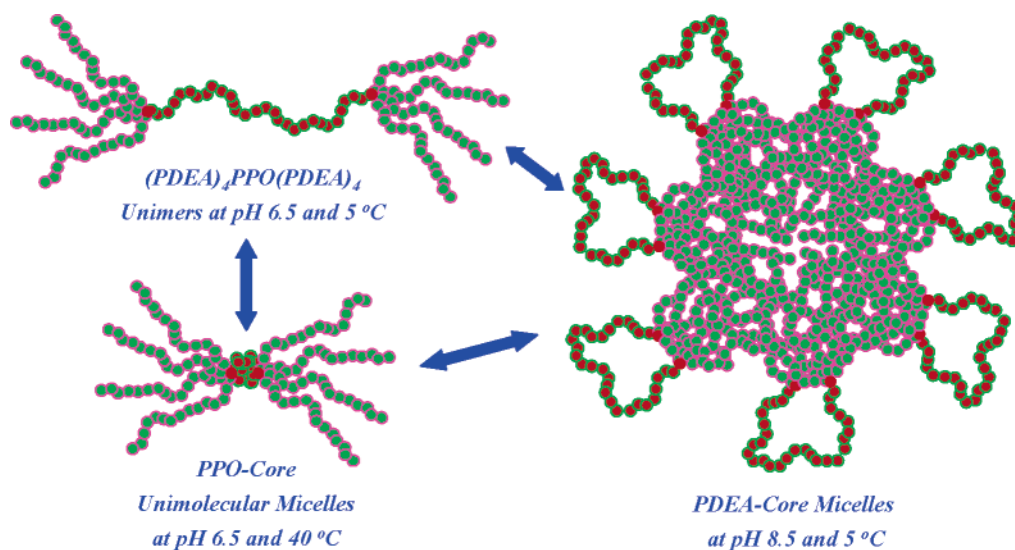


**Figure 6.** Schematic illustration of the micellization behavior of (PDEA)<sub>4</sub>PPO (PDEA)<sub>4</sub> of the star-*b*-linear-*b*-star type. Unimers, PPO-core unimolecular micelles, and PDEA-core micelles are formed at different solution conditions.



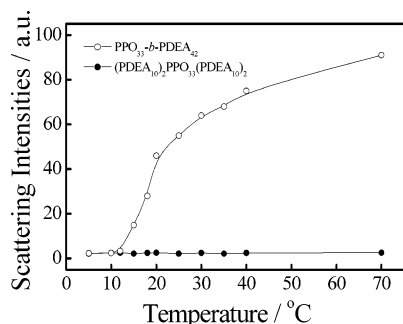


**Figure 7.** Variation of light scattering intensities as a function of temperature for the PPO<sub>33</sub>-b-PDEA<sub>42</sub> and (PDEA<sub>10</sub>)<sub>2</sub>PPO<sub>33</sub>(PDEA<sub>10</sub>)<sub>2</sub> block copolymers at a concentration of 0.5 wt % and pH 6.50.

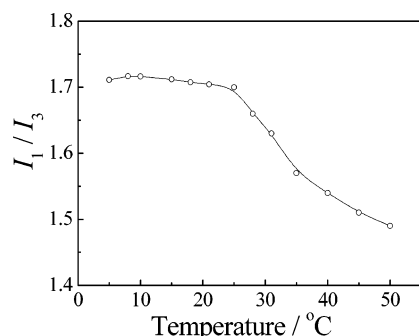


**Figure 8.** Temperature dependence of the  $I_1/I_3$  ratio for the (PDEA<sub>10</sub>)<sub>2</sub>-PPO<sub>33</sub>(PDEA<sub>10</sub>)<sub>2</sub> block copolymer at a concentration of 0.5 wt % and pH 6.5. The pyrene concentration is  $5 \times 10^{-7}$  M.

eters. Previously, <sup>1</sup>H NMR was employed to study the micellization of PPO-*b*-PDEA linear diblock copolymer, PPO block forming the micellar core typically exhibited weakened and broadened NMR signals.<sup>45</sup> When the (PDEA<sub>10</sub>)<sub>2</sub>PPO<sub>33</sub>(PDEA<sub>10</sub>)<sub>2</sub> solution in D<sub>2</sub>O (1.0 wt %, pH 6.5) was heated to 50 °C, the <sup>1</sup>H NMR signals of PPO residues showed negligible changes compared to that at 20 °C. This was probably due to that only unimolecular micelles were formed and no chain entanglements existed inside the micellar core. The thermoresponsive micellization behavior of (PDEA<sub>10</sub>)<sub>2</sub>PPO<sub>33</sub>(PDEA<sub>10</sub>)<sub>2</sub> at pH 6.5 was then further studied with fluorescence technique employing pyrene as a probe. Pyrene has been widely used as a probe of structure and dynamics in macromolecular systems because of its long excited-state lifetime and spectral sensitivity to the polarity of the surrounding medium.<sup>52</sup> In the emission spectra of the pyrene, the  $I_1/I_3$  ratio of the intensities of the first and third vibronic peaks was used to monitor the formation of hydrophobic microdomains. A decrease in  $I_1/I_3$  reflects the transfer of pyrene from a hydrophilic to a more hydrophobic microenvironment.

If unimolecular micelles were formed at elevated temperatures for (PDEA<sub>10</sub>)<sub>2</sub>PPO<sub>33</sub>(PDEA<sub>10</sub>)<sub>2</sub>, the hydrophobic PPO core will tend to solubilize the hydrophobic pyrene probes. Figure 8 showed the temperature dependence of the  $I_1/I_3$  ratio for the aqueous solution of (PDEA<sub>10</sub>)<sub>2</sub>PPO<sub>33</sub>(PDEA<sub>10</sub>)<sub>2</sub> at pH 6.5. In the temperature range 5–25 °C, the  $I_1/I_3$  ratio was  $\sim 1.7$ , indicating that the pyrene probe was located in a quite hydrophilic environment and thermoresponsive micellization did not occur. At temperatures  $> 25$  °C,  $I_1/I_3$  started to decrease. At 40 °C, this value was  $\sim 1.5$ . The inflection point (25 °C) of the  $I_1/I_3 \sim T$  curve can thus be ascribed to the critical micellization temperature. The above results suggested that the PPO central block of (PDEA<sub>10</sub>)<sub>2</sub>PPO<sub>33</sub>(PDEA<sub>10</sub>)<sub>2</sub> started to become hydrophobic and collapse at temperatures above 25 °C, and unimolecular micelles with the core consisting of a single

PPO block were thus formed. For (PDEA<sub>11</sub>)<sub>4</sub>PPO<sub>33</sub>(PDEA<sub>11</sub>)<sub>4</sub>, similar fluorescence measurements were conducted and the critical micellization temperature was determined to be  $\sim 35$  °C at a polymer concentration of 0.5 wt % and pH 6.5. This further confirmed that the decrease of  $I_1/I_3$  with temperature was not due to pyrene itself because the inflection point can vary with polymer chain architectures.

## Conclusions

Nonlinear-shaped double hydrophilic block copolymers (DHBCs) of the A<sub>2</sub>BA<sub>2</sub> and A<sub>4</sub>BA<sub>4</sub> type were synthesized for the first time and their micellization behavior was studied. Atom transfer radical polymerization (ATRP) macroinitiators with two and four initiating sites at both ends of the poly(propylene oxide) (PPO) chain were synthesized at first. Well-defined H-shaped (PDEA)<sub>2</sub>PPO(PDEA)<sub>2</sub> and (PDEA)<sub>4</sub>PPO(PDEA)<sub>4</sub> star-*b*-linear-*b*-star block copolymers were then prepared by polymerizing 2-(diethylamino)ethyl methacrylate (DEA) via ATRP in 2-propanol at 40 °C using the multifunctional macroinitiators, where PDEA was poly(2-(diethylamino)ethyl methacrylate). The pH-responsive and thermoresponsive micellization behavior of (PDEA<sub>10</sub>)<sub>2</sub>PPO(PDEA<sub>10</sub>)<sub>2</sub> and (PDEA<sub>11</sub>)<sub>4</sub>PPO(PDEA<sub>11</sub>)<sub>4</sub> was then investigated by a combination of dynamic laser light scattering and fluorescence techniques. At pH 8.5 and 5 °C, H-shaped (PDEA<sub>10</sub>)<sub>2</sub>PPO<sub>33</sub>(PDEA<sub>10</sub>)<sub>2</sub> and (PDEA<sub>11</sub>)<sub>4</sub>PPO<sub>33</sub>(PDEA<sub>11</sub>)<sub>4</sub> star-*b*-linear-*b*-star block copolymers formed much larger PDEA-core micelles compared to the linear counterpart, PPO<sub>33</sub>-b-PDEA<sub>42</sub>. The formed PDEA-core micelles took a “flowerlike” structure in which soluble PPO central block formed loops surrounding the insoluble PDEA core. In marked contrast to PPO<sub>33</sub>-b-PDEA<sub>42</sub>, upon heating the aqueous solutions at pH 6.4, both types of nonlinear block copolymers formed unimolecular micelles with the core consisting of a single PPO block. This was further confirmed by fluorescence measurements using pyrene as a probe.

**Acknowledgment.** This work was financially supported by an Outstanding Youth Fund (50425310) and a key research grant (20534020) from the National Natural Scientific Foundation of China (NNSFC), the “Bai Ren” Project of the Chinese Academy of Sciences, and the Program for Changjiang Scholars and Innovative Research Team in University (PCSIRT).

## References and Notes

- Colfen, H. *Macromol. Rapid Commun.* **2001**, *22*, 219–252.
- Butun, V.; Billingham, N. C.; Armes, S. P. *J. Am. Chem. Soc.* **1998**, *120*, 11818–11819.
- Rodriguez-Hernandez, J.; Lecommandoux, S. *J. Am. Chem. Soc.* **2005**, *127*, 2026–2027.
- Maeda, Y.; Mochiduki, H.; Ikeda, I. *Macromol. Rapid Commun.* **2004**, *25*, 1330–1334.
- Arotcarena, M.; Heise, B.; Ishaya, S.; Laschewsky, A. *J. Am. Chem. Soc.* **2002**, *124*, 3787–3793.
- Virtanen, J.; Arotcarena, M.; Heise, B.; Ishaya, S.; Laschewsky, A.; Tenhu, H. *Langmuir* **2002**, *18*, 5360–5365.
- Andre, X.; Zhang, M. F.; Muller, A. H. E. *Macromol. Rapid Commun.* **2005**, *26*, 558–563.
- Schilli, C. M.; Zhang, M. F.; Rizzardo, E.; Thang, S. H.; Chong, Y. K.; Edwards, K.; Karlsson, G.; Muller, A. H. E. *Macromolecules* **2004**, *37*, 7861–7866.
- Gil, E. S.; Hudson, S. A. *Prog. Polym. Sci.* **2004**, *29*, 1173–1222.
- Alarcon, C. D. H.; Pennadam, S.; Alexander, C. *Chem. Soc. Rev.* **2005**, *34*, 276–285.
- Dai, S.; Ravi, P.; Tam, K. C.; Mao, B. W.; Gang, L. H. *Langmuir* **2003**, *19*, 5175–5177.
- Gan, L. H.; Ravi, P.; Mao, B. W.; Tam, K. C. *J. Polym. Sci., Part A: Polym. Chem.* **2003**, *41*, 2688–2695.
- Butun, V.; Liu, S.; Weaver, J. V. M.; Bories-Azeau, X.; Cai, Y.; Armes, S. P. *React. Funct. Polym.* **2006**, *66*, 157–165.



- (14) Liu, S. Y.; Armes, S. P. *Angew. Chem., Int. Ed.* **2002**, *41*, 1413–1416.
- (15) Liu, S. Y.; Armes, S. P. *Langmuir* **2003**, *19*, 4432–4438.
- (16) Thomas, D. B.; Vasilieva, Y. A.; Armentrout, R. S.; McCormick, C. L. *Macromolecules* **2003**, *36*, 9710–9715.
- (17) Poe, G. D.; McCormick, C. L. *J. Polym. Sci., Part A: Polym. Chem.* **2004**, *42*, 2520–2533.
- (18) Sumerlin, B. S.; Lowe, A. B.; Thomas, D. B.; Convertine, A. J.; Donovan, M. S.; McCormick, C. L. *J. Polym. Sci., Part A: Polym. Chem.* **2004**, *42*, 1724–1734.
- (19) Hamley, I. W. *The Physics of Block Copolymers*; Oxford University Press: Oxford, U.K., 1998.
- (20) Mountrichas, G.; Mpiri, M.; Pispas, S. *Macromolecules* **2005**, *38*, 940–947.
- (21) Pispas, S.; Hadjichristidis, N.; Potemkin, I.; Khokhlov, A. *Macromolecules* **2000**, *33*, 1741–1746.
- (22) Hadjichristidis, N.; Iatrou, H.; Pitsikalis, M.; Pispas, S.; Avgeropoulos, A. *Prog. Polym. Sci.* **2005**, *30*, 725–782.
- (23) Iatrou, H.; Willner, L.; Hadjichristidis, N.; Halperin, A.; Richter, D. *Macromolecules* **1996**, *29*, 581–591.
- (24) Cai, Y. L.; Armes, S. P. *Macromolecules* **2005**, *38*, 271–279.
- (25) Cai, Y. L.; Tang, Y. Q.; Armes, S. P. *Macromolecules* **2004**, *37*, 9728–9737.
- (26) Hadjichristidis, N.; Pitsikalis, M.; Iatrou, H. *Adv. Polym. Sci.* **2005**, *189*, 1–124.
- (27) Hadjichristidis, N.; Pitsikalis, M.; Pispas, S.; Iatrou, H. *Chem. Rev.* **2001**, *101*, 3747–3792.
- (28) Knauss, D. M.; Huang, T. Z. *Macromolecules* **2002**, *35*, 2055–2062.
- (29) Knauss, D. M.; Huang, T. Z. *Macromolecules* **2003**, *36*, 6036–6042.
- (30) Hakiki, A.; Young, R. N.; Mcleish, T. C. B. *Macromolecules* **1996**, *29*, 3639–3641.
- (31) Haraguchi, N.; Hirao, A. *Macromolecules* **2003**, *36*, 9364–9372.
- (32) Lee, J. S.; Quirk, R. P.; Foster, M. D. *Macromolecules* **2005**, *38*, 5381–5392.
- (33) Hawker, C. J.; Bosman, A. W.; Harth, E. *Chem. Rev.* **2001**, *101*, 3661–3688.
- (34) Chiefari, J.; Chong, Y. K.; Ercole, F.; Krstina, J.; Jeffery, J.; Le, T. P. T.; Mayadunne, R. T. A.; Meijs, G. F.; Moad, C. L.; Moad, G.; Rizzardo, E.; Thang, S. H. *Macromolecules* **1998**, *31*, 5559–5562.
- (35) Chong, Y. K.; Le, T. P. T.; Moad, G.; Rizzardo, E.; Thang, S. H. *Macromolecules* **1999**, *32*, 2071–2074.
- (36) Wang, J. S.; Matyjaszewski, K. *Macromolecules* **1995**, *28*, 7901–7910.
- (37) Matyjaszewski, K.; Xia, J. H. *Chem. Rev.* **2001**, *101*, 2921–2990.
- (38) Li, Y. G.; Shi, P. J.; Pan, C. Y. *Macromolecules* **2004**, *37*, 5190–5195.
- (39) Han, D. H.; Pan, C. Y. *J. Polym. Sci., Part A: Polym. Chem.* **2006**, *44*, 2794–2801.
- (40) Xu, K.; Wang, Y.; Wang, Y. X.; Yu, T.; An, L. J.; Pan, C. Y.; Bai, R. *Polymer* **2006**, *47*, 4480–4484.
- (41) Liu, J.; Pan, C. Y. *Polymer* **2005**, *46*, 11133–11141.
- (42) Yu, X. F.; Shi, T. F.; Zhang, G.; An, L. J. *Polymer* **2006**, *47*, 1538–1546.
- (43) Durmaz, H.; Karatas, F.; Tunca, U.; Hizal, G. *J. Polym. Sci., Part A: Polym. Chem.* **2006**, *44*, 3947–3957.
- (44) Whittaker, M. R.; Urbani, C. N.; Monteiro, M. J. *J. Am. Chem. Soc.* **2006**, *128*, 11360–11361.
- (45) Liu, S. Y.; Billingham, N. C.; Armes, S. P. *Angew. Chem., Int. Ed.* **2001**, *40*, 2328–2331.
- (46) Liu, S. Y.; Armes, S. P. *J. Am. Chem. Soc.* **2001**, *123*, 9910–9911.
- (47) Mori, H.; Lanzendorfer, M. G.; Muller, A. H. E.; Klee, J. E. *Langmuir* **2004**, *20*, 1934–1944.
- (48) Mori, H.; Lanzendorfer, M. G.; Muller, A. H. E.; Klee, J. E. *Macromolecules* **2004**, *37*, 5228–5238.
- (49) Mori, H.; Muller, A. H. E.; Klee, J. E. *J. Am. Chem. Soc.* **2003**, *125*, 3712–3713.
- (50) Matyjaszewski, K. *Prog. Polym. Sci.* **2005**, *30*, 858–875.
- (51) Gohy, J. F. *Adv. Polym. Sci.* **2005**, *190*, 65–136.
- (52) Winnik, F. M. *Chem. Rev.* **1993**, *93*, 587–614.

MA061934W